



Research Paper

Non-Darcy flow and thermal radiation in convective embankment modeling



Marc Lebeau ^{*}, Jean-Marie Konrad

Department of Civil and Water Engineering, Laval University, Canada

ARTICLE INFO

Article history:

Received 13 August 2015

Received in revised form 18 November 2015

Accepted 26 November 2015

Available online 22 December 2015

Keywords:

Embankment

Natural convection

Non-Darcy flow

Thermal radiation

ABSTRACT

The design of convective embankments generally hinges on the use of numerical models that describe buoyancy-driven flow and heat transfer in porous media. A review of the literature reveals that most of the models used in the study of convective embankments assume that heat transfer occurs by conduction and convection, and that airflow can be described with Darcy's law. This is inconsistent with recent experimental evidence that suggests that radiative heat transfer is significant, and that Darcy's law does not adequately describe the relation between superficial flux and gradient in rockfill materials. In response to these shortcomings, a new model is herein derived to account for both radiative heat transfer and non-Darcy effects. After demonstrating its ability to solve fairly complex steady-state problems, the model is used to gain insight into the relative importance of radiative heat transfer and non-Darcy flow on the thermal response of a typical railway embankment. The radiative heat transfer is shown to be greater during the summer months. This increases the temperature at the base of the embankment, which in turn, increases the wintertime convective heat transfer. This additional heat extraction does not counteract the effect of the radiative heat transfer, and the wintertime temperatures below the embankment are shown to be warmer than that computed without radiative and non-Darcy effects.

© 2015 Elsevier Ltd. All rights reserved.

1. Introduction

The growing necessity for natural resources has prompted a renewed interest in Arctic and sub-Arctic regions, and led to the development of new transportation corridors. The design of the transportation lines within these corridors is challenged by the presence of permafrost, which is sensitive to minor changes in heat transfer at the ground surface. Overlooking the effect of these man-made structures on the surface heat balance can result in significant thaw, and settlement of the underlying permafrost. Over the years, a number of techniques have been proposed to mitigate the effect of embankment construction on thaw settlement. These techniques include the use of air ducts, thermosyphons, and convective embankments that enhance wintertime heat extraction. In this latter technique, the embankments are specifically engineered to enhance the wintertime heat extraction that occurs as convection currents cool the underlying permafrost. The design

of these convective embankments unavoidably hinges on our understanding of buoyancy-driven flow and heat transfer in coarse-grained porous media. This knowledge has been integrated into a number of numerical models for studying the behavior of convective embankments in permafrost-laden regions of Canada [1–3], China [4–9], and the United States of America [10–12]. All of these models assume that heat transfer occurs by conduction and convection, and most consider that airflow can be described with Darcy's law. This is inconsistent with recent experimental evidence that suggests that radiative heat transfer is significant, and that Darcy's law does not adequately describe the relation between superficial flux and gradient in coarse-grained soils. More precisely, Fillion et al. [13] determined the effective (combined conductive and radiative) thermal conductivity of four samples of crushed-rock with effective particle diameters ranging from 0.09 to 0.15 m. The effective thermal conductivity at ambient temperatures was found to be 97–209% greater than that ascribed to heat conduction. The effective thermal conductivity was also shown to increase with increasing effective particle diameter. These findings are consistent with the limits of predominant heat transfer mechanisms, shown in Fig. 1, which suggest that both radiative and convective heat transfer prevail in dry, coarse-grained, porous media. Zhang et al. [15], on the other hand, determined the airflow

^{*} Corresponding author at: Department of Civil and Water Engineering, Faculty of Sciences and Engineering, Adrien-Pouliot Pavilion, 1065, avenue de la Médecine, Laval University, Quebec, QC G1V 0A6, Canada. Tel.: +1 418 656 2131x3179; fax: +1 418 656 5343.

E-mail addresses: Marc.Lebeau@gci.ulaval.ca (M. Lebeau), Jean-Marie.Konrad@gci.ulaval.ca (J.-M. Konrad).

Nomenclature

a	absorption coefficient (L^{-1})	Pr	Prandtl dimensionless number
b	scattering coefficient (L^{-1})	q_a	volumetric flux of air (LT^{-1})
B	width of the enclosure and reference dimension (L)	\vec{q}_a	volumetric flux vector of air (LT^{-1})
C_F	dimensionless form-drag constant	\bar{q}_a	mean magnitude of the volumetric flux of air (LT^{-1})
C_t	volumetric heat capacity of the soil at constant pressure ($ML^{-1}T^{-2}\Theta^{-1}$)	q_r	radiative heat flux (MT^{-3})
$C_{t,a}$	volumetric heat capacity of air at constant pressure ($ML^{-1}T^{-2}\Theta^{-1}$)	\vec{q}_r	radiative heat flux vector (MT^{-3})
$C_{t,f}$	volumetric heat capacity of the frozen soil at constant pressure ($ML^{-1}T^{-2}\Theta^{-1}$)	R	radiative coefficient
$C_{t,u}$	volumetric heat capacity of the unfrozen soil at constant pressure ($ML^{-1}T^{-2}\Theta^{-1}$)	Ra	Rayleigh–Darcy dimensionless number
C_t^a	apparent volumetric heat capacity of the soil ($ML^{-1}T^{-2}\Theta^{-1}$)	Re	Reynolds dimensionless number
d_{10}	effective particle diameter (L)	S_r	degree of saturation
D	particle diameter (L)	t	time (T)
F	Forchheimer coefficient	T	absolute temperature (Θ)
g	gravitational acceleration constant (LT^{-2})	T_a	absolute ambient air temperature (Θ)
\vec{g}	gravity vector (LT^{-2})	T_o	reference absolute temperature (Θ)
Gr	Grashof dimensionless number	T_L	absolute temperature of fusion (liquidus) of pore water (Θ)
H	height of the enclosure (L)	T_S	absolute temperature of solidification (solidus) of pore water (Θ)
H_t	volumetric enthalpy ($ML^{-1}T^{-2}$)	T_1, T_2	absolute temperature of different surfaces (Θ)
k_t^e	effective thermal conductivity ($MLT^{-3}\Theta^{-1}$)	T_{s-1}, T_{s-2}	absolute temperatures at the upper boundaries of the railway embankment (Θ)
\bar{k}_t^e	mean effective thermal conductivity ($MLT^{-3}\Theta^{-1}$)	u_a	pore-air pressure ($ML^{-1}T^{-2}$)
k_t^c	conductive component of effective thermal conductivity ($MLT^{-3}\Theta^{-1}$)	$u_{a,o}$	reference pore-air pressure ($ML^{-1}T^{-2}$)
k_t^r	radiative component of effective thermal conductivity ($MLT^{-3}\Theta^{-1}$)	w	soil-freezing curve shape parameter
$k_{t,a}^c$	thermal conductivity of air ($MLT^{-3}\Theta^{-1}$)	x, z	spatial coordinates (L)
$k_{t,f}^c$	conductive component of the effective thermal conductivity of the frozen soil ($MLT^{-3}\Theta^{-1}$)	α_R	Roseland mean absorption coefficient (L^{-1})
$k_{t,u}^c$	conductive component of the effective thermal conductivity of the unfrozen soil ($MLT^{-3}\Theta^{-1}$)	β_o	reference volumetric thermal expansion coefficient of air (T^{-1})
K	intrinsic permeability (L^2)	ΔT	applied temperature differential (Θ)
\bar{K}	apparent permeability (L^2)	ε	emissivity of the surface
\bar{K}	mean apparent permeability (L^2)	$\varepsilon_1, \varepsilon_2$	emissivity of different surfaces
L	long-range radiation transmission parameter	θ_a	volumetric fraction of air
L_f	volumetric latent heat of fusion of water ($ML^{-1}T^{-2}$)	θ_w	volumetric fraction of liquid water
\bar{Nu}	mean Nusselt dimensionless number	$\theta_{w,f}$	volumetric fraction of liquid water in the frozen soil
		$\theta_{w,u}$	volumetric fraction of liquid water in the unfrozen soil
		$\mu_{a,o}$	reference dynamic viscosity of air ($ML^{-1}T^{-1}$)
		ρ_a	density of air (ML^{-3})
		$\rho_{a,o}$	reference density of air (ML^{-3})
		ρ_d	dry density (ML^{-3})
		σ	Stefan–Boltzmann constant ($MT^{-3}\Theta^{-4}$)

characteristics of four samples of crushed-rock with effective particle diameters ranging from 0.07 to 0.22 m. The tests were conducted in a wind tunnel, and yielded nonlinear relations between the superficial flux and gradient. These relations were shown to conform to the Darcy–Forchheimer law, which accounts for both viscous and inertial effects.

In response to these shortcomings, the paper proposes a new model for studying the behavior of convective embankments that accounts for both non-Darcy and radiative effects. The capabilities of the model are assessed with widely used benchmarks for natural convection in a shallow enclosure. The paper then establishes the importance of non-Darcy flow and radiative heat transfer on the response of a typical railway embankment.

2. Numerical model

2.1. Theory

The general mechanisms through which heat is transferred in convective embankments are conduction, convection, radiation, and phase changes. Heat conduction occurs as hot, rapidly moving or vibrating atoms and molecules transfer their energy to

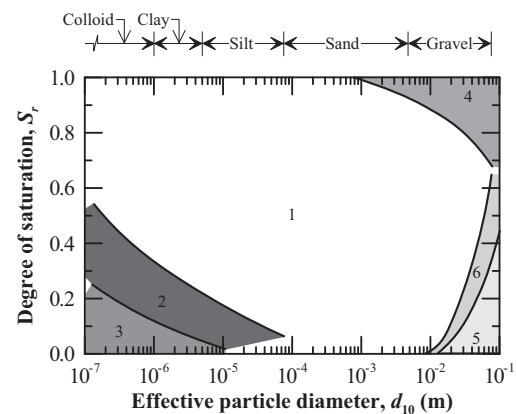


Fig. 1. Heat transfer mechanisms in porous media (Adapted from Johansen [14]). 1 – Conduction. 2 – Latent heat transfer by water vapor diffusion. 3 – Sensible heat transfer by water vapor diffusion. 4 – Natural convection (pore water). 5 – Natural convection (pore air). 6 – Radiation.

neighboring particles. It may also involve a rearrangement of water hydrogen bonds. Heat convection, on the other hand, occurs as pore fluid moves within the porous media. More precisely, forced

Download English Version:

<https://daneshyari.com/en/article/254575>

Download Persian Version:

<https://daneshyari.com/article/254575>

[Daneshyari.com](https://daneshyari.com)